

# Characterization of liquid phase mixing in turbulent bed contactor through RTD studies

A.E.R. Bruce, P.S.T. Sai, K. Krishnaiah\*

*Department of Chemical Engineering, Indian Institute of Technology Madras, Chennai 600036, India*

Received 7 January 2004; accepted 9 June 2004

---

## Abstract

Liquid phase mixing in a turbulent bed contactor (TBC) is experimentally characterized through residence time distribution (RTD) studies. A novel technique is employed to obtain the true exit tracer concentration and to increase the average residence time of the liquid. In this technique, an ideal mixed flow tank (MFT) is included in series with TBC. The RTD of the ideal MFT is deconvoluted from the RTD of the entire system to obtain the RTD of TBC alone. Using this method, the effect of gas and liquid velocities, static bed height, particle size and density, and number of stages on mixing of the liquid phase is studied. The experimental RTD curves are satisfactorily compared with axial dispersion model. Correlations are developed for predicting the Peclet number and the axial dispersion coefficient. It is observed in the present study that conditions close to plug flow of liquid phase can be achieved in multistage TBC.

© 2004 Elsevier B.V. All rights reserved.

*Keywords:* Multiphase flow; Multiphase reactors; Fluidization; Turbulent bed contactor; Dispersion; Axial mixing

---

## 1. Introduction

Turbulent bed contactor (TBC) is a gas–liquid–solid fluidized bed with liquid trickling down through an expanded bed of solids supported by the gas flowing counter-current to the liquid. TBC finds extensive applications for many physical, chemical and biochemical processes such as air cooling, humidification, particulate removal, flue gas desulfurization, absorption, scrubbing and alcohol fermentation [1]. The chief advantages of TBC are its ability to operate at large gas and liquid throughputs without plugging and high heat and mass transfer rates. Successful design and operation of TBC requires, apart from hydrodynamic information, the knowledge of the effect of various parameters that influence the axial mixing of the phases as increased axial mixing reduces the driving force for heat and mass transfer.

Bruce et al. [2] reviewed the work reported on liquid phase mixing in TBC. They mentioned the shortcomings of the experimental techniques employed by the earlier investigators.

Most of them placed the conductivity cell below the distributor plate to measure the exit tracer concentration. Since liquid falls down throughout the cross section of the distributor plate, the location of the probe used by them may not represent the true tracer concentration. In addition to this, the average residence time of liquid in the column is very short and hence prone to errors in measurement of residence time distribution (RTD). Bruce et al. [2] studied the liquid phase mixing in TBC by providing a downcomer for routing the liquid from one stage to another. The presence of downcomer enhances the gas throughput in the column. Under these conditions, the problem with probe location was not faced as the probe was directly placed in the downcomer to measure the true concentration of the tracer. While most of the reported information on liquid phase mixing is restricted to single stage TBC, no information is available on multistage TBC.

In order to overcome the difficulties in obtaining the true tracer concentration and to increase the average residence time of the liquid, a novel technique is attempted in the present study. In this technique, the liquid phase mixing is obtained through RTD studies by incorporating an ideal mixed flow tank (MFT) in series with the TBC [3]. Since the RTD of the

---

\* Corresponding author.

*E-mail address:* krishnak@iitm.ac.in (K. Krishnaiah).

## Nomenclature

$d_p$	diameter of particle (m)
$D_c$	column diameter (m)
$D_e$	axial dispersion coefficient ( $m^2/s$ )
$E(t)$	exit age distribution function ( $s^{-1}$ )
$E(\theta)$	dimensionless exit age distribution function
$H$	height of the expanded bed (m)
$H_0$	static bed height (m)
$N$	number of stages
$P$	$Pe/4$
$Pe$	Peclet number
$T_1, T_2$	as defined in Eq. (5)
$u_g$	superficial gas velocity (m/s)
$u_l$	superficial liquid velocity (m/s)
$u_{mf}$	minimum fluidization velocity (m/s)

### Greek letters

$\theta$	dimensionless residence time ( $t/\tau$ )
$\lambda$	root of transcendental equation
$\tau$	average residence time (s)

ideal MFT is known, it can be deconvoluted from the RTD of the entire system to obtain the RTD of TBC alone. This technique increases the average residence time of the liquid and solves the problem of positioning of conductivity probe as the probe can be inserted in the outlet of MFT. Using this technique, the effects of gas and liquid flow rates, static bed height and particle size and density on the liquid phase axial mixing is studied in TBC operated in Type I mode (particle density  $< 300 \text{ kg}^3$ ). An attempt is also made to study the residence time distribution of liquid phase in multistage TBC to characterize its mixing.

During the earlier studies [4] on TBC, it was observed that some of the liquid sprayed at the top of the column was sliding down along the wall and through the distributor without contacting the solid and gas phases. Hence to minimize the channeling of liquid and to improve the contact between the phases, the holes of the distributor near the wall are blocked with a projection of the gasket into the column. In the present work, all the experimental data on liquid phase mixing are collected with a gasket projection of 3 mm. Bruce et al. [5] described the details of the projection.

## 2. Experimental

The details of the experimental setup of the TBC were described elsewhere [5]. The column was made of Perspex with an i.d. of 113 mm and an o.d. of 122 mm using multiple sections. The total height of the column including the collection tank at the bottom and the entrainment section at the top was 3.22 m. The collection tank had 161 mm i.d. and a height of

Table 1  
Range of variables

Variable	Range
Gas velocity, $u_g$ ( $m \text{ s}^{-1}$ )	2–5
Liquid velocity, $u_l$ ( $m \text{ s}^{-1}$ )	0–0.0042
Static bed height, $H_0$ (m)	0.07, 0.107, 0.147
Distributor plate free open area, $f$	0.70
Particle diameter, $d_p$ (m)	0.012, 0.016, 0.025
Particle density, $\rho_p$ ( $\text{kg m}^{-3}$ )	110, 145, 215
Number of stages, $N$	1, 2, 3

366 mm, which was connected to a MFT of 2.4 liter capacity. The liquid from MFT is collected in a tank which is connected to the storage tank. The concentration of the tracer is measured by means of an on-line conductivity measurement in which a conductivity probe is inserted near the outlet of the MFT. The details of data collection are described elsewhere [2].

At a particular set of chosen parameters, a known liquid flow rate was sent into the column counter-current to a particular gas flow rate. After the column attains steady state conditions, a known volume of the tracer (5 N NaCl) is injected as pulse just above the liquid distributor in a very short time (less than  $(1/10)$  of a second). The concentration of the tracer was recorded using the online conductivity probe and data acquisition system. The experimental procedure is repeated for various gas and liquid flow rates, static bed heights and particle characteristics such as particle size and density. The range of the variables of the present study is listed in Table 1.

## 3. Results and discussion

### 3.1. RTD of empty column with MFT

If the RTD data of empty column with MFT is deconvoluted from the RTD data of TBC in series with the MFT, the RTD data due to TBC alone can be obtained. Hence a separate set of experiments was conducted at different gas and liquid flow rates to obtain the RTD of empty column with MFT and these experiments indicated that the behavior of the system is close to perfectly mixed flow tank. These data were obtained by smoothing the original experimental data with splines of suitable tension factors using the MATLAB<sup>®</sup> function 'csaps' are used for deconvolution. A typical experimentally obtained exit age distribution,  $E(\theta)$  against  $\theta$  of empty column with MFT, is shown in Fig. 1.

### 3.2. RTD of TBC with MFT

The RTD of the liquid phase in TBC with MFT is obtained for different gas and liquid velocities, static bed heights and particle density and diameter. Fig. 2 shows a typical exit age distribution curve. These data were deconvoluted using Brenner model [6] proposed for large axial dispersion with closed-closed boundary conditions.

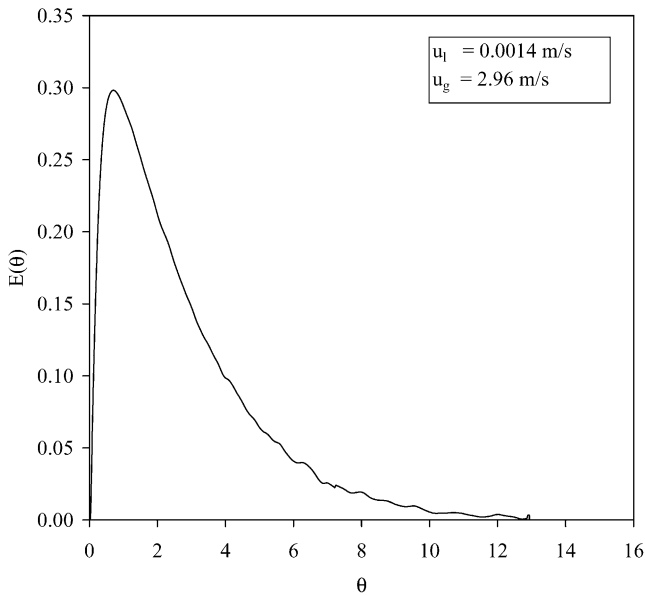


Fig. 1. Exit age distribution of liquid phase in empty column with MFT.

### 3.3. RTD of TBC

The deconvolution procedure employed in the present study is similar to that proposed by Michelsen [7] and is as follows:

$$E_{out}(t) = \int_0^t f(\tau, Pe) E_{in}(t - \tau) d\tau \quad (1)$$

where  $E_{out}(t)$  is the smoothed data for TBC with MFT,  $E_{in}(t)$  is the smoothed RTD data for empty column with MFT,  $f(\tau, Pe)$  is the axial dispersion model impulse response function of TBC alone.

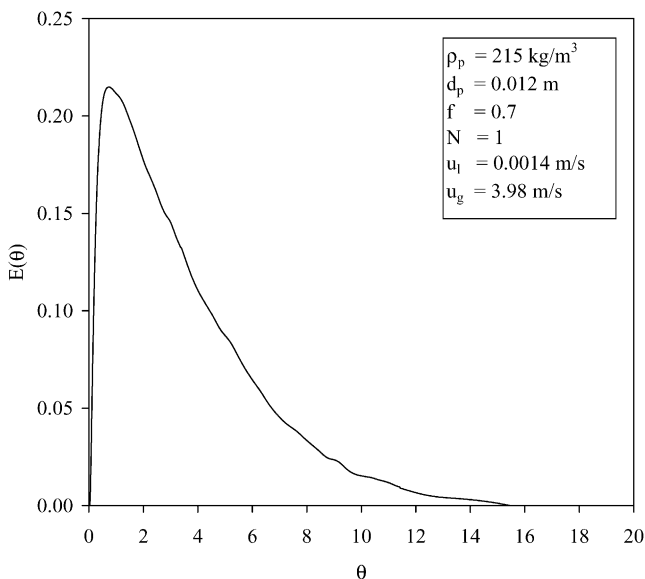


Fig. 2. RTD of liquid phase in TBC with MFT.

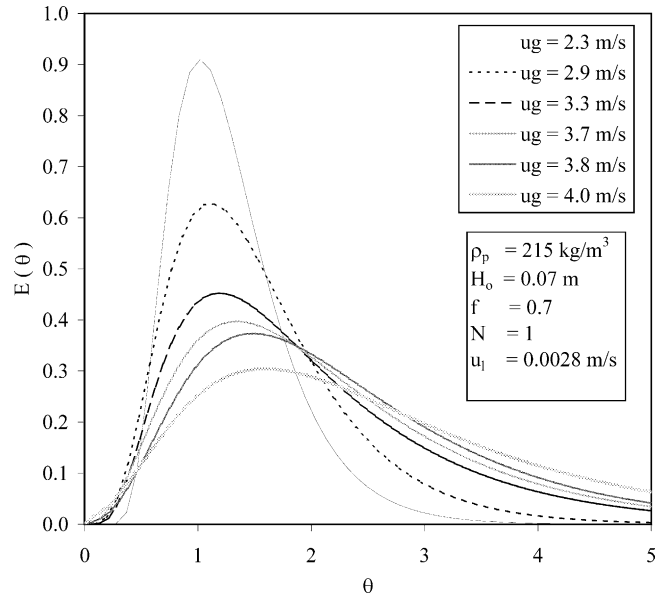


Fig. 3. Effect of gas velocity on mixing.

The optimal values of the parameters  $Pe$  and  $\tau$  are obtained by least square minimization of objective function (using the function ‘leastsq’ in MATLAB®)

$$J = \sum (E_{out} - E_{outpred})^2 \quad (2)$$

The  $Pe$  and  $\tau$  obtained by the above procedure are used to obtain the RTD of the system (TBC) from the equation of the axial dispersion model with closed-closed boundary condition given by Brenner [6].

### 3.4. Effect of operating parameters on mixing

The dimensionless exit age distribution for TBC at various gas velocities is shown in Fig. 3. It can be seen from the figure that the mixing of liquid phase increases with increase in gas velocity as evident from the spread in the RTD curves. At higher gas velocities, the solids move rapidly in the bed and increase the turbulence in the liquid phase. The same trend was observed by Chen and Douglas [8] and Rama et al. [9] for TBC without downcomer and Bruce et al. [2] with downcomer.

The effect of liquid velocity on RTD of liquid phase is shown in Fig. 4. The trend is similar to that reported by Bruce et al. [2] for system with downcomer. At a given gas velocity, an increase in liquid velocity increases the liquid holdup which in turn contributes for more backmixing in the system due to the stirring effect of gas on the liquid in the presence of solids. It is seen that the mixing increases with increase in packing size as shown in Fig. 5. As particle diameter increases, the gas velocity required to fluidize also increases causing more mixing in the liquid phase. In Type I TBC, the liquid holdup is not affected by particle density [5,10] and hence, the effect of particle size is shown in Fig. 5, even though each particle has a different density.

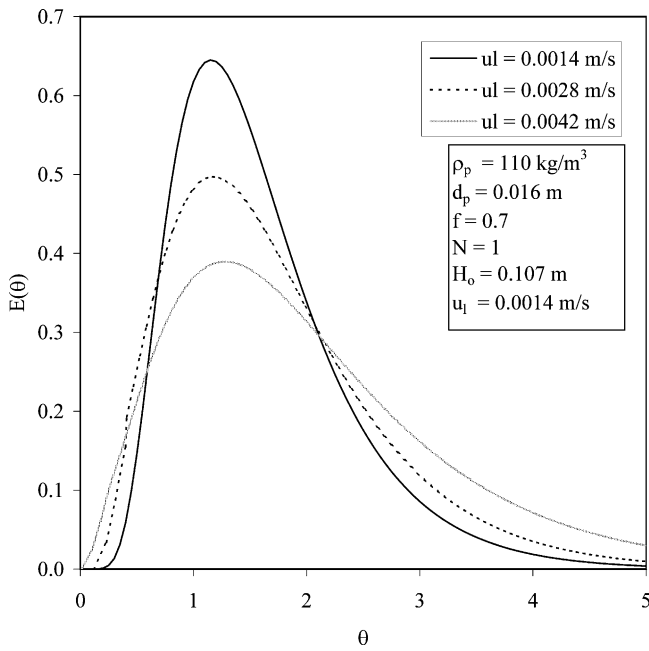


Fig. 4. Effect of liquid velocity on mixing.

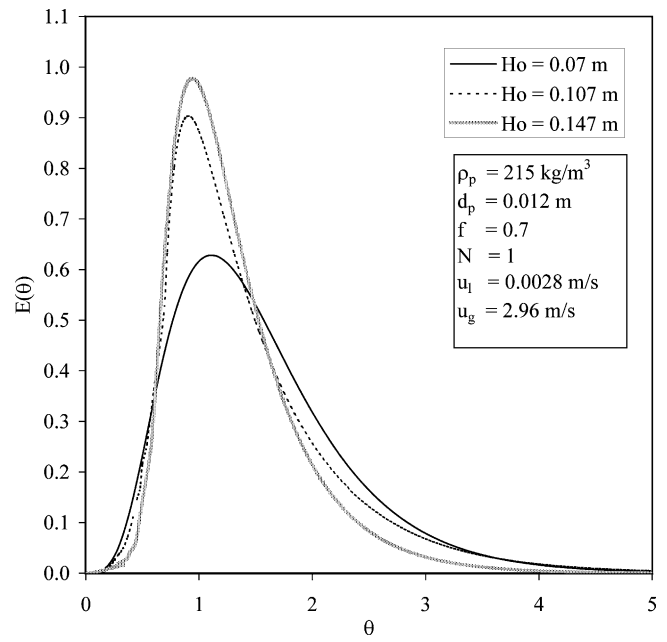


Fig. 6. Effect of static bed height on mixing.

The effect of static bed height on liquid phase mixing is shown in Fig. 6. At a fixed gas velocity, as the static bed height increases the movement of the particles decreases thus decreasing the mixing of liquid in the bed. Increase in static bed height, on the other hand, increases the number of particles in a given volume and to accommodate the extra volume of the particles the system adjust with less amount of liquid in the bed.

In the present study, RTD data of liquid phase was obtained on single, two and three stages. At fixed velocities of gas and

liquid, the effect of increase in number of stages is shown in Fig. 7. As expected, the mixing decreases with increase of number of stages taking the system towards the plug flow. This observation is consistent with that of Bruce at al. [2] for system with downcomer. This can be explained with the analogy of the increase in number of mixed flow reactors in series taking the system towards plug flow. This is because the bypassing fraction of liquid from first stage need not bypass second and third stages. On the whole if one has infinite numbers of stages, all fractions of liquid phase spend the

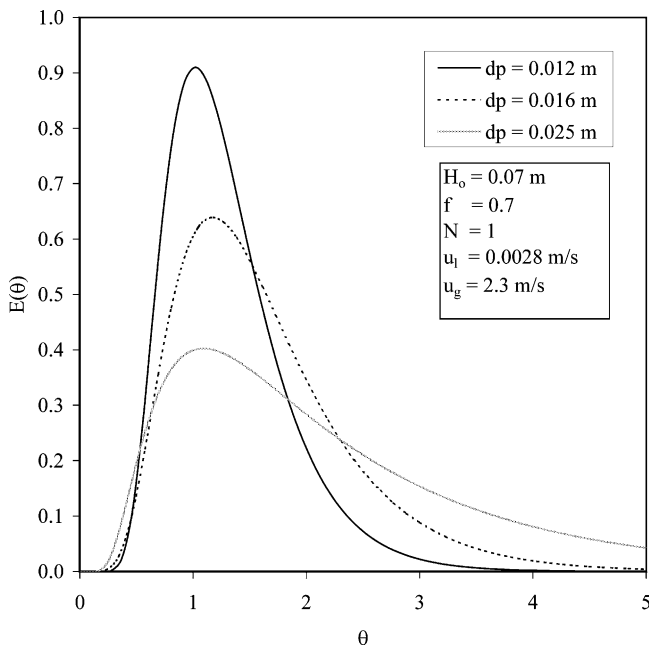


Fig. 5. Effect of particle diameter on mixing.

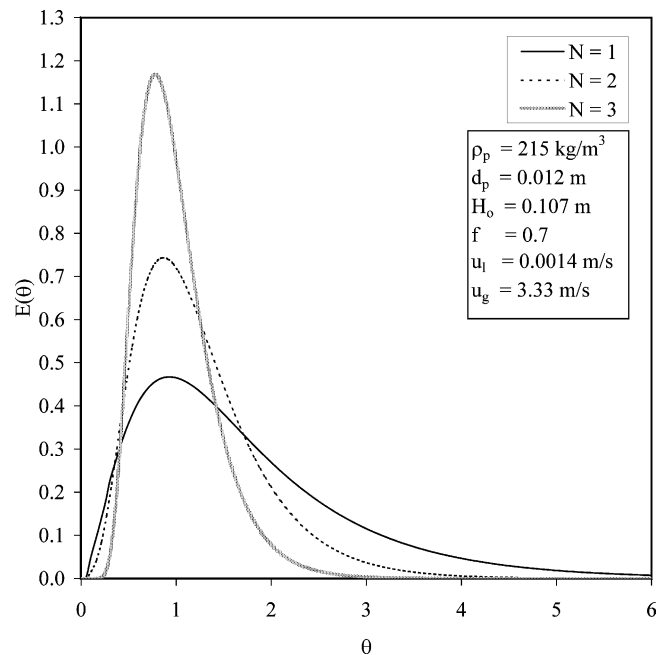


Fig. 7. Effect of number of stages on mixing.

same residence time which satisfies the definition of plug flow.

### 3.5. Estimation of Peclet number

The RTD of liquid phase in empty column without MFT of the present study suggests that the system is close to plug flow. Hence, it is confirmed that the liquid is in plug flow before and after the mobile bed. Therefore, the TBC can be considered as a closed-closed system [3]. In determining the axial liquid phase mixing, dispersion model was used taking into account the physical phenomenon of the system [8,9]. The experimental RTD data collected in the present work are characterized using Brenner model [6], which is the only model available for large dispersion with closed-closed boundary conditions. Since the present experimental setup corresponds to closed-closed boundary with large dispersion, this model was chosen to represent the RTD and to evaluate the Peclet numbers.

Bruce et al. [2] derived the following equations for  $E(\theta)$  for general (Eq. (3)) and asymptotic (Eq. (4)) solutions:

$$E(\theta) = \frac{\exp(2P - P\theta)}{P} \times \sum_{k=1}^n \frac{\lambda_k \sin(2\lambda_k) \exp(-\lambda_k^2 \theta / P) (\lambda_k^2 + P^2)}{(\lambda_k^2 + P^2 + P)} \quad (3)$$

$$E(\theta) = \left(\frac{\theta P}{4\pi}\right)^{1/2} \exp\left[-\frac{P(1-\theta)^2}{\theta}\right] \left[\frac{1+\theta}{\theta^2}\right] + \left[\frac{dT_1}{d\theta}\right] - \exp(4P) \left[\frac{dT_2}{d\theta}\right] \quad (4)$$

where

$$\left[\frac{dT_1}{d\theta}\right] = \frac{1}{2\theta^2} \left(\frac{4P\theta}{\pi}\right)^{1/2} \exp\left[-\frac{P(1-\theta)^2}{\theta}\right] \times \left[4P^2(1+\theta-\theta^2-\theta^3) + P(6+2\theta) + 3\theta\right]$$

$$\left[\frac{dT_2}{d\theta}\right] = \left[\frac{1}{2} + 2P(3+4\theta) + 4P^2(1+\theta^2)\right] \times \left[\frac{4P\theta}{\pi}\right]^{1/2} \exp\left[-\frac{P(1+\theta)^2}{\theta}\right] \frac{(1-\theta)}{2\theta^2} + \operatorname{erfc}\left[\left(\frac{P}{\theta}\right)^{1/2}(1+\theta)\right] \left[8P + 8P^2(1+\theta)\right] \quad (5)$$

Following the procedure described by Bruce et al. [2], theoretical curves are generated using Eqs. (3) and (4) and the Peclet numbers are evaluated for all the experimental runs. Chen and Douglas [8] used only the first term of Eq. (3) and estimated the Peclet number after converting it to linear form. Rama et al. [9] used Eq. (3) for comparing theoretical with

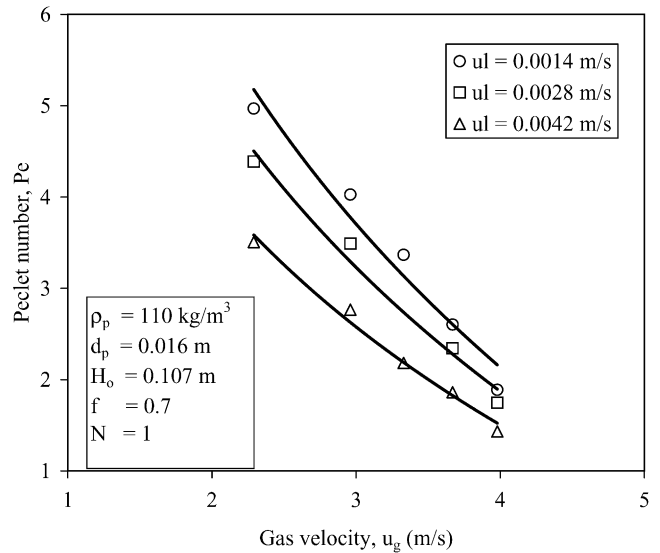


Fig. 8. Effect of gas and liquid velocities on Peclet number.

the experimental curve and calculated the Peclet number from the second moment of the experimental curve. Bruce et al. [2] used asymptotic equation for obtaining the theoretical RTD curve. While the former two investigators conducted their studies without downcomer, the later is with the downcomer.

### 3.6. Effect of operating parameters on Peclet number

The effect of gas velocity on Peclet number is shown in Fig. 8. It can be seen from the figure that the Peclet number decreases with increase in gas velocity which is due to the increase in turbulence of liquid with intense circulations, thus enhancing the mixing in the liquid phase. As the liquid velocity increases, the holdup in the system increases which creates more turbulence with the passage of the gas, i.e. the presence of more liquid within the bed reduces the void space which in turn increases the interstitial gas velocity causing the random motion of the particles. This decreases the Peclet number as can be seen from Fig. 8 in which the effect of liquid flow rate is also shown. The variation in Peclet number with particle size is shown in Fig. 9. As the particle size increases the fluidizing velocity increases, intensifying the local motion of the particles, enhancing liquid phase mixing, thus decreasing the Peclet number.

Fig. 9, which also shows the effect of static bed on Peclet number, indicates that Peclet number increases with static bed height. With increase in bed height, the number of particles in the bed increases thus limiting the movement of particles in the bed and results in decrease in mixing (high Peclet number). The effect of number of stages on Peclet number is shown in Fig. 10. As expected, the Peclet number increases with increase in number of stages, taking the system towards plug flow behavior. These observations are, in general, similar to systems with downcomer [2].

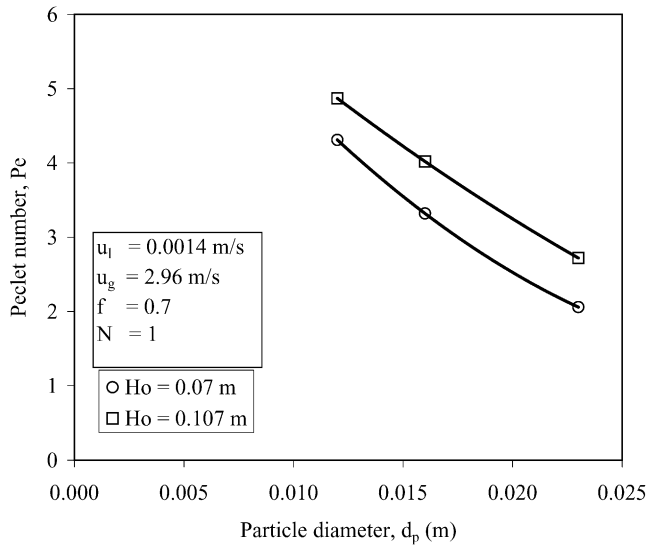


Fig. 9. Effect of particle diameter and static bed height on Peclet number.

### 3.7. Effect of operating parameters on axial dispersion coefficient

The axial dispersion coefficient, an important parameter for characterization of mixing, is evaluated from the experimentally determined Peclet number as follows:

$$D_e = \frac{H^2}{\tau Pe} \quad (6)$$

The variation of axial dispersion coefficient, with gas velocity is shown in Fig. 11. From the figure, it can be seen that axial dispersion coefficient increases with increase in gas velocity, indicating that mixing of liquid in the system increases. The effect of higher gas velocity being displayed more strongly, as seen from Fig. 11, where the movement of

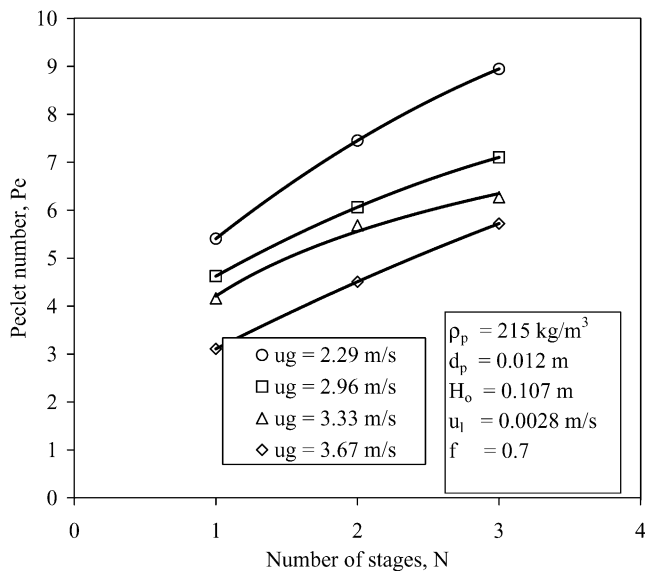


Fig. 10. Effect of number of stages on Peclet number.

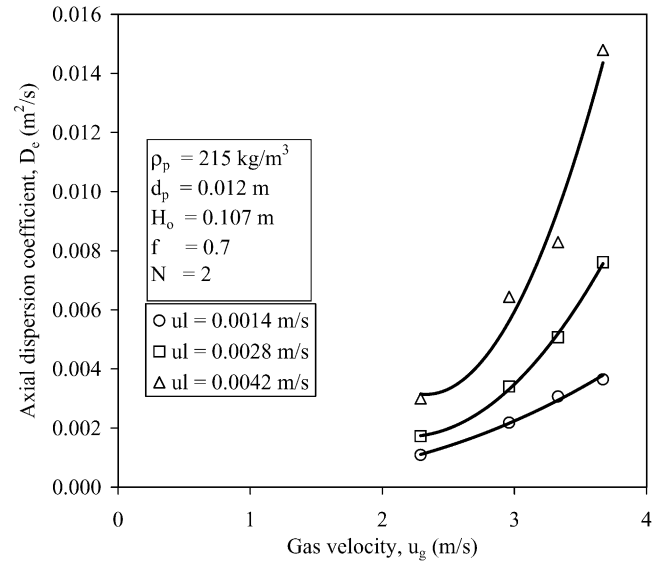


Fig. 11. Effect of gas and liquid velocities on axial dispersion coefficient.

the phases is most intensive owing to the high kinetic energy of the gas. It can also be observed that at higher liquid rates ( $u_l = 0.0042$  m/s), the increase in axial dispersion coefficient is sharper (Fig. 11). With increase in liquid velocity, the axial dispersion coefficient increases indicating an increase in mixing at high liquid rates. As liquid velocity increases, the liquid held in the bed increases, thus reducing the open cross section (void space) for passage of gas and liquid flow. This is accompanied by increase in friction between gas and liquid which lead to increase in the amount of liquid in the bed causing high turbulence.

The variation of particle diameter on axial dispersion coefficient is shown in Fig. 12. The axial dispersion coefficient increases with increase of particle diameter. As the minimum

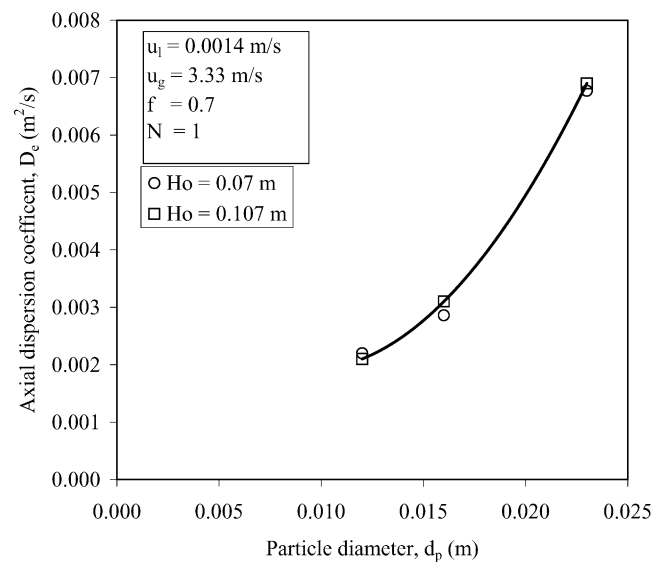


Fig. 12. Effect of particle diameter and static bed height on axial dispersion coefficient.



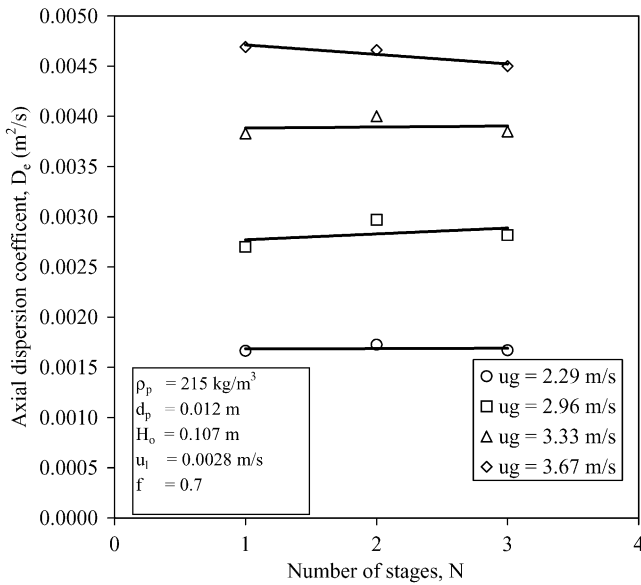


Fig. 13. Effect of number of stages on axial dispersion coefficient.

fluidization velocity increases with increase in diameter ( $u_{mf} \propto d_p$ ) the quantity,  $u_l - u_{mf}$  increases causing more mixing. The axial dispersion coefficient is almost independent of static bed height (Fig. 12). At a particular gas and liquid velocity with a fixed diameter of the particle, the expanded bed has the same voidage throughout the length. Then the interstitial velocity remains constant, which causes uniform dispersion. As static bed height increases, expanded bed height and Peclet number increase which causes the axial dispersion coefficient constant (Eq. (6)).

From Fig. 13, it can be seen that the axial dispersion coefficient remains almost constant with increase in number of stages. This is true because with increase in number of stages, the residence time distribution move towards plug flow, since Peclet number as well as total expanded bed height increases with increase in number of stages. Hence, in Eq. (6),  $D_e$  is almost constant.

### 3.8. Correlations

Based on the results obtained in the present study, correlations developed for Peclet number and axial dispersion coefficient covering a wide range of variables for Type I TBC are as follows:

$$Pe = 0.46u_g^{-1.07}u_l^{-0.23}d_p^{-0.55}H_0^{0.42}D_c^{-0.16}N^{0.68} \quad (7)$$

$$D_e = 10.46u_g^{0.92}u_l^{0.53}d_p^{0.22}D_c^{0.36} \quad (8)$$

Figs. 14 and 15 compare the experimental and predicted data of Peclet number and axial dispersion coefficient respectively. The prediction of Peclet number fits 87% of the experimental data with a RMS error of 28% and axial dispersion coefficient fits 80% of the experimental data with a RMS error of 23% respectively. The experimental data of Chen and Douglas [8], Rama et al. [9] and Koval et al. [11]

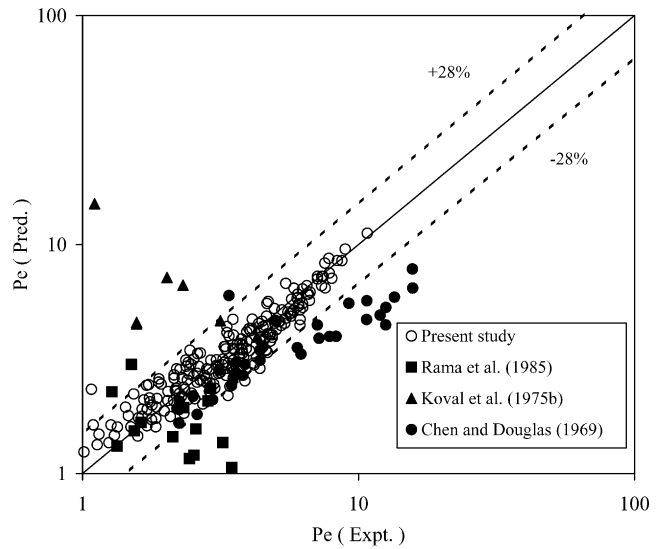


Fig. 14. Comparison of experimental and predicted Peclet numbers.

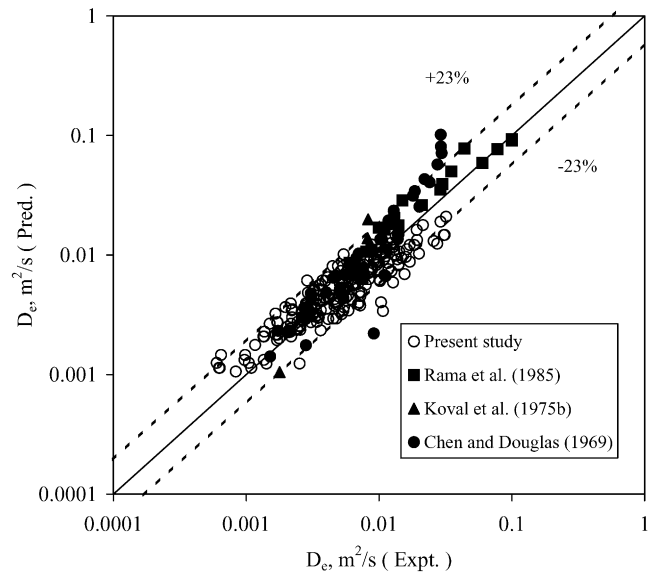


Fig. 15. Comparison of experimental and predicted axial dispersion coefficients.

are satisfactorily compared with the present correlations in these figures.

## 4. Conclusions

Based on the experimental RTD data, it is observed that mixing of liquid phase increases with increase in gas and liquid velocities, and particle diameter and decreases with increase in static bed height and number of stages. The Peclet number obtained through deconvolution decreases with increase in gas and liquid velocities, and particle diameter and increases with increase in static bed height and number of stages. The axial dispersion coefficient calculated us-

ing  $\tau$ ,  $Pe$  and expanded bed height increases with increase in gas and liquid velocities, and particle diameter and is independent of both static bed height and number of stages. Correlations are proposed to predict satisfactorily Peclet number and axial dispersion coefficients of liquid phase in TBC.

## References

- [1] L.S. Fan, Gas–Liquid–Solid Fluidization Engineering, Butterworths, London, MA, USA, 1989.
- [2] A.E.R. Bruce, P.S.T. Sai, K. Krishnaiah, Chem. Eng. Sci. 58 (2003) 3453–3463.
- [3] O. Levenspiel, Chemical Reaction Engineering, second ed., Wiley Eastern, New Delhi, 1972.
- [4] K. Soundarajan, Hydrodynamics of Single and Multi-Stage Turbulent Bed Contactor with and without Downcomer, Ph.D. Thesis, Indian Institute of Technology Madras, Chennai, 1995.
- [5] A.E.R. Bruce, P.S.T. Sai, K. Krishnaiah, Chem. Eng. J. 99 (2004) 203–212.
- [6] H. Brenner, Chem. Eng. Sci. 17 (1962) 229.
- [7] M.L. Michelsen, Chem. Eng. J. 4 (1972) 171.
- [8] B.H. Chen, W.J.M. Douglas, Can. J. Chem. Eng. 47 (1969) 113.
- [9] O.P. Rama, D.P. Rao, V. Subba Rao, Can. J. Chem. Eng. 63 (1985) 443.
- [10] G.V. Vunjak-Novakovic, D.V. Vukovic, H. Littman, Ind. Eng. Chem. Res. 26 (5) (1987) 958.
- [11] Z.A. Koval, A.V. Beshpalov, O.G. Kuleshov, A.P. Zhukov, Theor. Found. Chem. Eng. 9 (1975) 837.